Rollover Index for the Diagnosis of Tripped and Untripped Rollovers

Abstract

It is necessary to detect danger as soon as possible to avoid rollover of a vehicle in sudden events. Using rollover index in real time can be used for this purpose. The traditional rollover indices currently applying in the vehicles can only detect the untripped rollover due to severe lateral acceleration in vehicles. These indices cannot detect the tripped rollover resulted from vertical external forces in a long direction. There are recently many quantitative studies about the tripped rollover and an index was also introduced to this kind of rollover. In this research, we examined the dynamics of a SUV to improve this index and also presented a new index to detect the both types of rollovers. The precision and accuracy of the new index was evaluated by simulation in industrial software of Carsim. The numerical results of the new developed model were compared with the test results of an automobile at one-eighth scale in equal conditions and inputs. The results are indicative of the better performance of the new model presented in this research.

Amir Hossein Kazemian [a,*]
Majid Fooladi [b]
Hossein Darijani [c]

[a] Mechanical Engineering Department, University of Sistan and Baluchestan, Zahedan, Iran. kazemian@eng.usb.ac.ir
[b] Mechanical Engineering Department, Shahid Bahonar University of Kerman, Kerman, Iran. fooladi@uk.ac.ir
[c] Mechanical Engineering Department, Shahid Bahonar University of Kerman, Kerman, Iran. darijani@uk.ac.ir

* Corresponding Author

1 INTRODUCTION

As the dimensions of vehicles increase, they are more possible to have rollover in different road conditions. The rollover may occur in one of two ways: tripped or untripped. Untripped rollover results from the high lateral acceleration in sharp turnings of road. On the other hand, tripped rollover may occur as a result of external vertical forces applied to the automobile
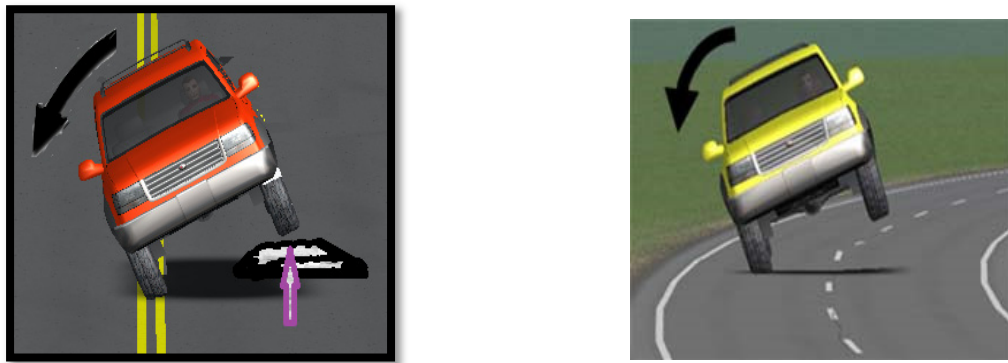
a) Tripped Rollover	b) Untripped Rollover

Figure 1: Types of rollover.

Automobile rollovers considerably contribute to deathful driving accidents. In about 11 million accidents in passenger car, SUV, pickup and vans in 2010, only 3 percent of the accidents were related to the rollover. However, close to 33 percent of all the mortality caused by accidents is resulted from rollover(National Highway Traffic and Safety Board, 2011). Based on information published by NHTSA in 2006, the accidents caused by rolling were observed in 70% of light vehicle accidents. Thus, in recent years, rollover is considered as an important safety issue for vehicles.
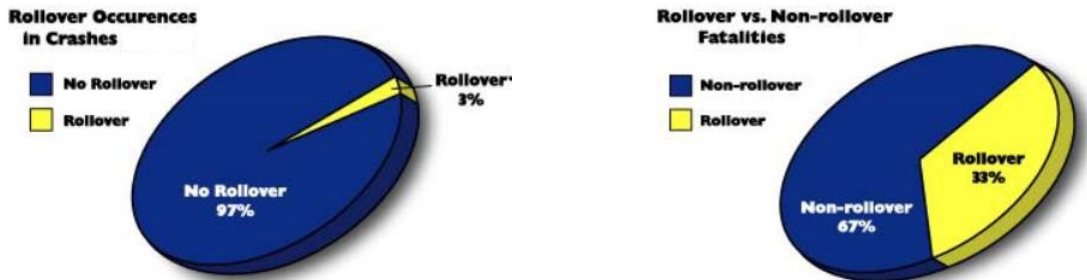
Figure 2: Statistical results of NHTSA (Phanomchoeng & Rajamani, 2012).

Given the increasing interests of costumers in Sport Utility Vehicle (SUV) in recent years, many automobile companies are also interested in production of these kinds of automobiles. There is a great range of factors affecting the rollover of these cars, including variety of maneuver, driving conditions, road situation, geometry of car, and car performance. To detect the rollover, it is necessary to define an index or scale to measure the stability of the automobile. The index gives the possibility to the controller to make judgments about the possibility of rollover and send the appropriate command (Peters, 2006). Each of the indices is calculated by input data from sensors and dynamic state of the vehicle. It is necessary to measure the value by some predefined program values as rollover thresholds. The first and most basic indicator that shows the inherent tendency of a vehicle to overturn and usually comes from static test conditions is named static stability factor

(SSF)(Dilich & John, 1997). It can also be used in roll angle as an index to detect the rollover, but it is not used as an independent index and usually applied as a supplementary factor (Hsu & Chen, 2012). Another important and useful criterion is automobile energy index. In this index, the kinetic energy of the vehicle is compared with the maximum amount of potential energy and its dynamics is controlled before it reaches this threshold (Johansson & Gafvert, 2004). Another index that is defined on the basis of forces between the tire and road is the index lateral load transfer. To determine the index, the vertical force of left and right tires is calculated and if their difference passes the threshold, the controller is activated(R Rajamani, Piyabongkarn, Tsourapas, & Lew, 2009). Based on the angle between the tire contact force and road surface, rollover index is defined as a measure force-angle. Based on the mentioned criteria, various new indices can be created. For example, the criterion Time to Rollover (TTR) is defined based on roll angle and lateral pressure(Chen & Peng, 1999; Yoon, Kim, & Yi, 2007).

Selecting one of the rollover indices, vehicle dynamic stability can be obtained through the use of different control methods. Many researches presented a variety of mechanisms including different suspension systems (Cech, 2000), differential braking system, and steering control mechanism activated by using different control methods in order to control vehicle rollover. Solmaz et al.(Solmaz, Corless, & Shorten, 2007) presented a method based on discrete-time systems in active steering control to analyze rolling dynamics of vehicles. Tavan et al. (2015) proposed an optimal controller for integrated longitudinal and lateral closed loop vehicle dynamics to follow desired path in various driving maneuvers (Tavan, Tavan, & Hosseini, 2015). The design of a suspension system emphasizes weight reduction (Kong, Abdullah, Omar, & Haris, 2016) Active and semi-active suspension systems are kinds of automotive suspension mechanisms that control cyclic vertical movement of the car in a broad frequency range and energy waste through real-time feedback. Every moment the tires go up and down separately depending on the conditions of the road until the car's occupants will have the maximum comfort(Solmaz, Shorten, Wulff, & Cairbre, 2008).Pagnacco et al. designed an active suspension device to satisfy certain limitations in a given frequency(Pagnacco, Zidani, Sampaio, de Cursi, & Ellaia, 2016; Pan, He, Xiao, & Liu, 2016).

In this research, in an innovation, by adding two symmetrically equal masses to a passive 4 degrees of freedom of a half vehicle suspension model (Rajesh Rajamani & Phanomchoeng, 2013) and also using magneto-rheological (MR) damper (Ahmadian, 2014), a hybrid semi active 6 degrees of freedom suspension system is designed. Thus, the dynamics equations of rollover index based on vertical forces between tires and the road is developed. To investigate the controllability of the system with increases in degrees of freedom, the hybrid semi-active suspension system with 8 degrees of freedom was designed in combination with the model of passive suspension system with 4 degrees of freedom and semi-active suspension system with 6 degrees of freedom. The new model with 8 degrees of freedom is based on the model with 6 degrees of freedom and two further masses were added to sprung part to make the model with 8 degrees of freedom. Finally, the new suspension models are modeled in Carsim application. The results of the simulation and those of the study (Rajesh Rajamani & Phanomchoeng, 2013)were compared under the same road conditions. The results have indicated that the system with 8 degrees of freedom has better performance and both the new systems can prevent a rollover accident.

2   VEHICLE ROLLOVER INDEX

Vehicle rollover index is a real-time variable that can be used for wheel lift-off conditions. The basic definition of rollover R is described as:

$$R = \frac{F_{zr} - F_{zl}}{F_{zr} + F_{zl}} \qquad -1 \leq R \leq 1 \tag{1}$$

Where F_{zr} and F_{zl} are the vertical force of right and left tires. When the vehicle is in a rollover threshold, the index value is greater than 1 or less than 1. It is noteworthy that when the automobile is moving in a straight road, both the F_{zr} and F_{zl} are equal and the rollover value is zero. As $F_{zl} = 0$, then R=1, and the vehicle just will be on the right tire on the surface. The relation 1 cannot be implemented because the forces are not measureable. Many attempts have been conducted by researchers to obtain the indices. Many of the attempts resulted in the index based on lateral acceleration and untripped rollover. An applied formula of R rollover index can be based on ϕ and a_y .

$$R_1 = \frac{2 m_s a_y h_R}{m g L_w} + \frac{2 m_s h_R \tan(\phi)}{m L_w} \tag{2}$$

Where $m = m_s + m_u$, h_R is the height of center gravity m_u is the unsprung mass, m_s is the sprung mass, a_y is the lateral acceleration, and ϕ is the rotation angle. This rollover index can just be applied to detect untripped rollover. Some studies defined the rollover index just based on lateral acceleration because it is difficult to find roll angle (Odenthal, Bunte, & Ackermann, 1999; Solmaz, Corless, & Shorten, 2006). The stability control with this index may reduce the ability of lateral movement of the vehicle and is not also able to detect the rollover resulted by vertical forces and road inputs.

$$R_2 = \frac{2 m_s a_y h_R}{m g L_w} \tag{3}$$

In commercial form of index, the acceleration of sprung mass is also considered separately (Rajesh Rajamani & Phanomchoeng, 2013).

$$R_3 = \frac{2 m_s a_y h_R}{m g L_w} + \frac{2 m_s h_R \tan(\phi)}{m L_w} + \frac{m_u \left(\ddot{z}_{ur} - \ddot{z}_{ul} \right)}{m g} \tag{4}$$

Where $\left(\ddot{z}_{ur} - \ddot{z}_{ul} \right)$ is the difference between the acceleration of unsprung masses.

For the first time Rajamani et al. (Phanomchoeng & Rajamani, 2013) in 2013 introduced rollover index based on vertical forces in accordance with Equation (5). The index is for cars with 4 degrees of freedom suspension systems, both for tripped and untripped rollover.
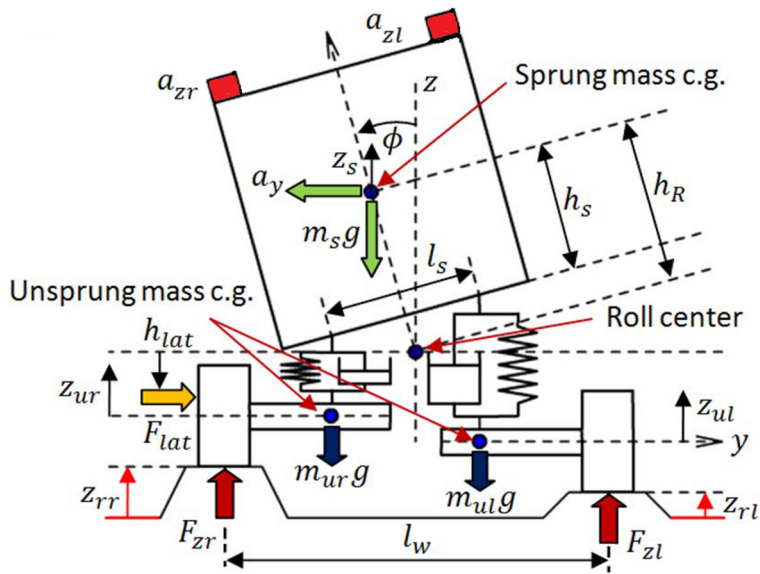
Figure 3: tripped and untripped rollover model in 4 degrees of freedom
suspension systems (Phanomchoeng & Rajamani, 2013).

$$R_4 = \frac{m_u\left(\ddot{z}_{ur} - \ddot{z}_{ul}\right) - \frac{2}{l_s^2}\left(I_{xx} + m_s h_R^2\right)\left(a_{zl} - a_{zr}\right) + \frac{2}{l_s}m_s h_R\left(a_y \cos(\phi) + g \sin(\phi)\right)}{m_u\left(\ddot{z}_{ur} + \ddot{z}_{ul}\right) + m_s \ddot{z}_s + \left(m_s + 2m_u\right)g} \tag{5}$$

Where $\left(a_{zl} - a_{zr}\right)$ is the difference between acceleration of sprung mass and I_{xx} is the roll moment of inertia around longitudinal axes.

According to the national highway safety administration (NHTSA), 95% of rollovers in single-seat vehicles are related to tripped rollover. Thus, development and improvement of these indicators have significant potential impact on technology.

Where $\left(a_{zl} - a_{zr}\right)$ is the difference between acceleration of sprung mass and I_{xx} is the roll moment of inertia around longitudinal axes.

According to the national highway safety administration (NHTSA), 95% of rollovers in single-seat vehicles are related to tripped rollover. Thus, development and improvement of these indicators have significant potential impact on technology.

3 IMPROVED ROLLOVER INDEX FOR TRIPPED AND UNTRIPPED ROLLOVERS

3.1 Rollover Index for 6 Degrees of Freedom Suspension Systems

In order to detect the untripped rollover due to external vertical forces, the rollover index should consider the effects of road forces. In this study, the suspension system with 6 degrees of freedom in analysis of vehicle rollover dynamics is introduced. Therefore, two symmetrical equal masses were added to unsprung parts of the suspension system with 4 degrees of freedom. This was to design a

hybrid semi-active suspension system of 6 degrees of freedom using a magneto-rheological damper (Ahmadian, 2014) (Figure 4).

It should be noted that adding degrees of freedom is a way to assess its impacts on stability and well controllability of the system. As represented in Figure 4, the m_{u_2} represents the masses added to the unsprung part of the automobile.

The 6 degrees of freedom suspension system in a vehicle is vertical movement of the sprung mass in z_s, rotation angle ϕ and vertical movements of right and left unsprung masses, $\left(z_{u_1r}, z_{u_1l}, z_{u_2r}, z_{u_2l} \right)$. Variables of z_{rr} and z_{rl} are road profiles that motivate the system and enter a lateral force input F_{lat} in a certain height h_{lat} from the center of rotation. The external outputs of z_{rr}, z_{rl} and F_{lat} cannot be measured and thus, are unknown. However, these outputs depending on these inputs can be measured. For example, lateral and vertical accelerations can be measured by different accelerometers. These lateral and vertical accelerations can be related to unknown inputs or algebraic equations. Figure 4 represents these forces ($\left(F_{zr}, F_{zl} \right)$).
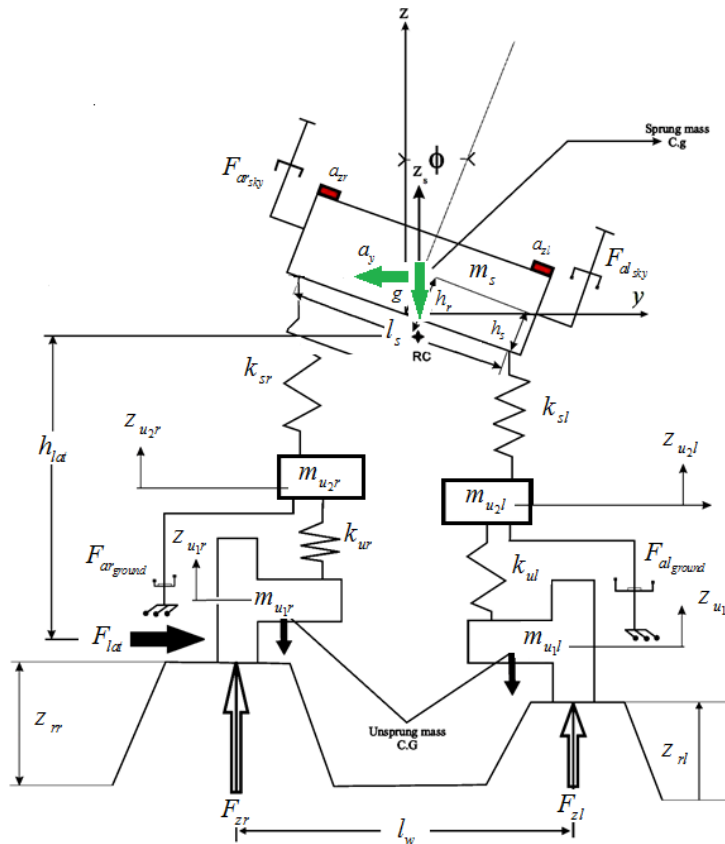
Figure 4: A semi-active hybrid 6 degrees of freedom suspension system.

The lateral forces exerted on the system can also be observed in Figure 5.
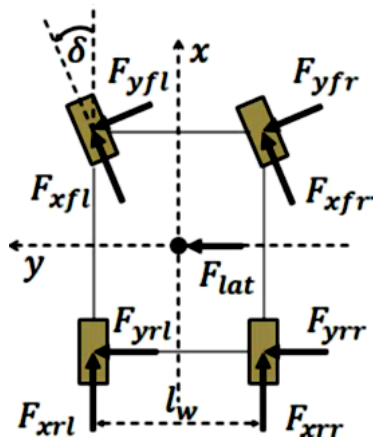
Figure 5: Lateral forces in schematic view.

$$a_y = \frac{\left(F_{yf} \cos\left(\delta\right) + F_{xf} \sin\left(\delta\right) + F_{yr} + F_{lat} \right)}{m} \tag{6}$$

In this figure, the value a_y is including of lateral tire forces and the unknown force of F_{lat} where, $m = m_s + \sum\limits_{i=1}^{2} m_{u_i r} + \sum\limits_{j=1}^{2} m_{u_j l}$ and F_{xf} is the longitudinal force in right and left fore-wheels, F_{yr} and F_{yf} are the lateral forces of back and fore tires s in right and left, and δ is the steering angle.

As the effects of road inputs are considered, the suspension forces on chassis are as follow:

$$F_{sr_{total}} = F_{sr_1} - F_{ar_{sky}} \tag{7}$$

$$F_{sl_{total}} = F_{sl_1} - F_{al_{sky}} \tag{8}$$

Where F_{sr_1} and F_{sl_1} are passive suspension system forces and $F_{ar_{sky}}$ and $F_{al_{sky}}$ are semi active damper forces of a vehicle.

$$F_{sr_1} = -k_{sr}\left(z_s - \frac{l_s}{2}\sin\left(\phi\right) - z_{u_2 r} \right) \tag{9}$$

$$F_{sl_1} = -k_{sl}\left(z_s - \frac{l_s}{2}\sin\left(\phi\right) - z_{u_2 l} \right) \tag{10}$$

This is noteworthy that magneto-rheological (MR) has been used and the direct impacts of this damper have been considered in a new index. Thus, the impacts of $F_{ar_{sky}}$ and $F_{al_{sky}}$ from the forces of F_{sr} and F_{sl} are also considered separately.

Applying the second principle of Newton law for the sprung mass leads to:

$$m_s \ddot{z}_s = F_{sr_1} + F_{sl_1} + F_{ar_{sky}} + F_{al_{sky}} - m_s g \tag{11}$$

Dynamic modeling of moving unsprung mass is carried out in two steps. First, the basic dynamic equations are added to the two objects of m_{u_2r}, m_{u_2l}, and then, it is added to unsprung mass of tires that are in direct contact with the ground.

Applying Newton's second law for the unsprung masses leads to:

$$m_{u_2r}\ddot{z}_{u_2r} = -F_{sr_1} + F_{u_1r} - m_{u_2r}g + F_{ar_{ground}} \tag{12}$$

As a result,

$$F_{u_1r} = m_{u_2r}\ddot{z}_{u_2r} + F_{sr_1} + m_{u_2r}g - F_{ar_{ground}} \tag{13}$$

Likewise, for the unsprung mass in left tire we have:

$$m_{u_2l}\ddot{z}_{u_2l} = -F_{sl_1} + F_{u_1l} - m_{u_2l}g + F_{al_{ground}} \tag{14}$$

Where,

$$F_{u_1l} = m_{u_2l}\ddot{z}_{u_2l} + F_{sl_1} + m_{u_2l}g - F_{al_{ground}} \tag{15}$$

Thus, the dynamic equations of movement for the unsprung masses of tires are:
In the right tire:

$$m_{u_1r}\ddot{z}_{u_1r} = -F_{u_1r} + F_{tr} - m_{u_1r}g \tag{16}$$

In the left tire:

$$m_{u_1l}\ddot{z}_{u_1l} = -F_{u_1l} + F_{tl} - m_{u_1l}g \tag{17}$$

By replacing the equations 13 and 14 in the equations 16 and 17, the result is:

$$m_{u_1r}\ddot{z}_{u_1r} = m_{u_2r}\ddot{z}_{u_2r} + F_{sr_1} + m_{u_2r}g + F_{tr} - m_{u_1r}g + F_{ar_{ground}} \tag{18}$$

$$m_{u_1l}\ddot{z}_{u_1l} = m_{u_2l}\ddot{z}_{u_2l} + F_{sl_1} + m_{u_2l}g + F_{tl} - m_{u_1l}g + F_{al_{ground}} \tag{19}$$

Therefore, for the new model in this study, the vertical forces can be calculated as:

$$F_{tr} = m_{u_1r}\ddot{z}_{u_1r} + m_{u_2r}\ddot{z}_{u_2r} + F_{sr_1} + m_{u_2r}g + m_{u_1r}g - F_{ar_{ground}} \tag{20}$$

$$F_{tl} = m_{u_1l}\ddot{z}_{u_1l} + m_{u_2l}\ddot{z}_{u_2l} + F_{sl_1} + m_{u_2l}g + m_{u_1l}g - F_{al_{ground}} \tag{21}$$

Since the vertical forces of F_{tr}, F_{tl} are equal to those of F_{zr}, F_{zl}, the rollover index is:

$$R_{6-DOF} = \frac{\begin{array}{l} m_{u_1r}\ddot{z}_{u_1r} + m_{u_2r}\ddot{z}_{u_2r} + \left(F_{sr_1} - F_{sl_1}\right) - m_{u_1l}\ddot{z}_{u_1l} - m_{u_2l}\ddot{z}_{u_2l} \\ + \left(m_{u_1r} + m_{u_2r} - m_{u_1l} - m_{ul_2}\right)g + \left(F_{al_{ground}} - F_{ar_{ground}}\right) \end{array}}{\begin{array}{l} m_{u_1r}\ddot{z}_{u_1r} + m_{u_2r}\ddot{z}_{u_2r} + \left(F_{sr_1} + F_{sl_1}\right) + m_{u_1l}\ddot{z}_{u_1l} + m_{u_2l}\ddot{z}_{u_2l} \\ + \left(m_{u_1r} + m_{u_2r} + m_{u_1l} + m_{ul_2}\right)g - \left(F_{ar_{ground}} + F_{al_{ground}}\right) \end{array}} \tag{22}$$

Where F_{sr_1}, F_{sl_1} are replaced with Equations (9) and (10). Given that the parameters of the forces are unknown and not easily measurable; this needs to remove the unknown parameters. Calculating the suspension system F_{sr_1}, F_{sl_1} by Equation (11) resulted in:

$$\left(F_{sr_1} + F_{sl_1}\right) = m_s\ddot{z}_s + m_s g - \left(F_{ar_{sky}} + F_{al_{sky}}\right) \tag{23}$$

The equation of rotation movement around the roll center (RC) leads to:

$$\left(I_{xx} + m_s h_R^2\right)\ddot{\phi} = \frac{l_s}{2}\left(F_{sl_1} - F_{sr_1}\right) + \frac{l_s}{2}\left(F_{al_{sky}} - F_{ar_{sky}}\right) + m_s a_y h_R \cos\phi + m_s g h_R \sin\phi \tag{24}$$

As a result,

$$\left(F_{sl_1} - F_{sr_1}\right) = \frac{2}{l_s}\left(\left(I_{xx} + m_s h_R^2\right)\ddot{\phi} - m_s g h_R \sin(\phi) - m_s a_y h_R \cos(\phi) - \frac{l_s}{2}\left(F_{al_{sky}} - F_{ar_{sky}}\right)\right) \tag{25}$$

The $\ddot{Z}_s$ parameter can be measured by an accelerometer. The ϕ angle can be calculated by a tilt angle sensor. One example of a tilt meter is the Crossbow CXTD02. This is consisted of two axis in-built accelerometers and a signal processing algorithm to calculate the angles of tilting. For example, one of the algorithms for this purpose is mentioned in (Rajesh Rajamani, 2011) . To calculate the $\ddot{\phi}$, two extra accelerometers are required to be placed at the right and left ends on an automobile sprung mass.
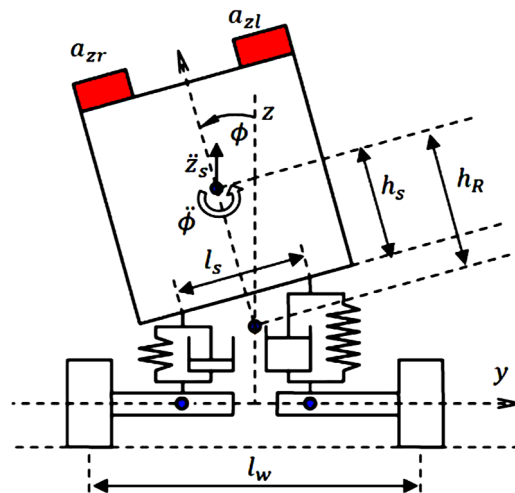
Figure 6: extra accelerometer position.

The value of the right accelerometer a_{zr} is obtained as:

$$a_{zr} = \ddot{z}_s \cos(\phi) - \frac{ls}{2}\ddot{\phi} + (\ddot{y} + v_x\dot{\psi})\sin(\phi) + g\cos(\phi) \tag{26}$$

The left accelerometer is also obtained as:

$$a_{zl} = \ddot{z}_s \cos(\phi) + \frac{ls}{2}\ddot{\phi} + (\ddot{y} + v_x\dot{\psi})\sin(\phi) + g\cos(\phi) \tag{27}$$

Where the component $(\ddot{y} + v_x\dot{\psi})$ is the effect of the unknown force F_{lat}.
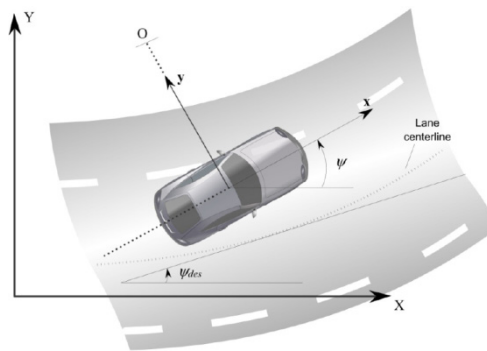
Figure 7: Schematic of lateral dynamics of a vehicle (Rajesh Rajamani, 2011).

By subtracting the equation 26 from the equation 27, we would reach:

$$(a_{zl} - a_{zr}) = l_s\ddot{\phi} \Rightarrow \ddot{\phi} = \frac{(a_{zl} - a_{zr})}{l_s} \tag{28}$$

By replacing Equations 23, 25, and 28 with Equation 22, the left and right masses are assumed to be equal, and the rollover index of the vehicle with 6 degree of freedom suspension system leads to:

$$R_{6-DOF} = \cfrac{m_{u_1}(\ddot{z}_{u_1r} - \ddot{z}_{u_1l}) + m_{u_2}(\ddot{z}_{u_2r} - \ddot{z}_{u_2l}) - \dfrac{2(I_{xx} + m_s h_R^2)}{l_s^2}(a_{zl} - a_{zr})}{\begin{array}{c} m_{u_1}(\ddot{z}_{u_1r} + \ddot{z}_{u_1l}) + m_{u_2}(\ddot{z}_{u_2r} + \ddot{z}_{u_2l}) + m_s\ddot{z}_s - \left(F_{ar_{sky}} + F_{al_{sky}}\right) \\ +2(m_{u_2} + m_{u_1} + \dfrac{m_s}{2})g - \left(F_{al_{ground}} + F_{ar_{ground}}\right) \end{array}}$$

$$+ \cfrac{\dfrac{2}{l_s}m_s h_R\left(a_y\cos(\phi) + g\sin(\phi)\right) + \left(F_{ar_{sky}} - F_{al_{sky}}\right) + \left(F_{al_{ground}} - F_{ar_{ground}}\right)}{\begin{array}{c} m_{u_1}(\ddot{z}_{u_1r} + \ddot{z}_{u_1l}) + m_{u_2}(\ddot{z}_{u_2r} + \ddot{z}_{u_2l}) + m_s\ddot{z}_s - \left(F_{ar_{sky}} + F_{al_{sky}}\right) \\ +2(m_{u_2} + m_{u_1} + \dfrac{m_s}{2})g - \left(F_{al_{ground}} + F_{ar_{ground}}\right) \end{array}} \tag{29}$$

3.2 Rollover Index for Automobile Suspension System with 8 Degrees of Freedom

To improve the stability and controllability of a suspension system with increasing degree of freedom, a new hybrid semi active suspension system with 8 degrees of freedom has been designed in combination with a semi-active hybrid suspension system with 6 degrees of freedom and a passive suspension system with 4 degrees of freedom. To do so, we added two symmetrical equal masses to the sprung part and also used MR damper of the hybrid suspension system with 8 degrees of freedom. As can be observed in Figure 8, m_{s_2} represents the added masses to the sprung part.
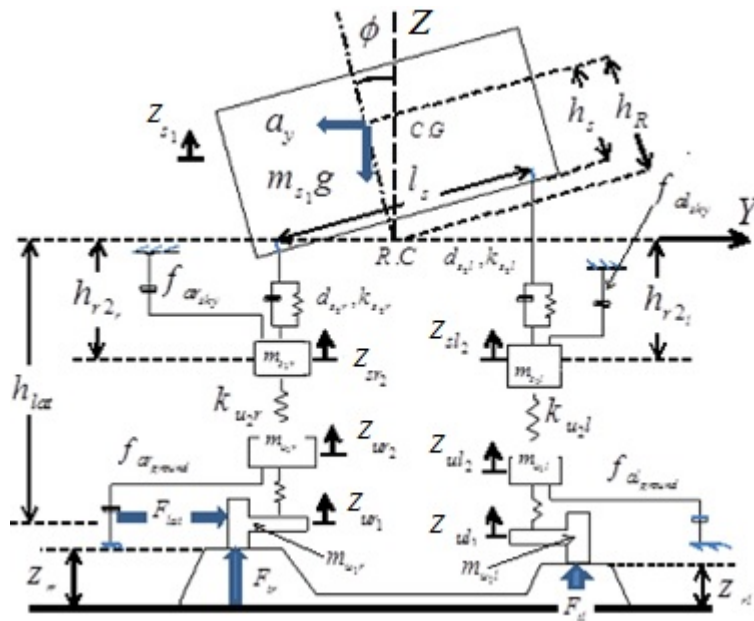
Figure 8: A hybrid semi-active 8 degrees of freedom suspension system.

According to the previous arguments and based on Equation 6, the value of lateral acceleration including the effects of lateral forces and the force of F_{lat} can be seen as:

$$a_y = \frac{\left(F_{yf}\cos(\delta) + F_{xf}\sin(\delta) + F_{yr} + F_{lat}\right)}{m} \tag{30}$$

Where $m = \sum m_s + \sum m_u$

The suspension forces exerted on the chassis include

$$F_{sr_{total}} = F_{sr} - F_{ar_{sky}} \tag{31}$$

$$F_{sl_{total}} = F_{sl} - F_{al_{sky}} \tag{32}$$

Where,

$$F_{sr} = -k_{sr}\left(z_{s_1} - \frac{l_s}{2}\sin(\phi) - z_{s_2r}\right) - d_{sr}\left(\dot{z}_{s_1} - \frac{l_s}{2}\dot{\phi}\cos(\phi) - \dot{z}_{s_2r}\right) \tag{33}$$

$$F_{sl} = -k_{sl}\left(z_{s_1} + \frac{l_s}{2}\sin(\phi) - z_{s_2l}\right) - d_{sl}\left(\dot{z}_{s_1} + \frac{l_s}{2}\dot{\phi}\cos(\phi) - \dot{z}_{s_2l}\right) \tag{34}$$

By assuming that the suspension forces always act vertically, the sprung mass 1 roll motion is given by:

$$\left(I_{xx} + m_{s_1}h_{R_1}^2\right)\ddot{\phi} = \frac{l_s}{2}\left(F_{sl} - F_{sr}\right) + \frac{l_s}{2}\left(F_{al_{sky}} - F_{ar_{sky}}\right) + m_{s_1}\,g\,h_{R1}\sin(\phi) + m_{s_1}a_y h_{R1}\cos(\phi) \tag{35}$$

By applying Newton's second law to the chassis:

$$m_{s1}\ddot{z}_{s_1} = F_{sr} + F_{sl} + F_{ar_{sky}} + F_{al_{sky}} - m_{s_1}g \tag{36}$$

Similarly, for the added sprung masses:

$$m_{s_2r}\ddot{z}_{s_2r} = -F_{sr} - F_{ar_{sky}} - m_{s_2r}g + k_{u_2r}\left(z_{s_2r} - z_{u_2r}\right) \tag{37}$$

$$m_{s_2l}\ddot{z}_{s_2l} = -F_{sl} - F_{al_{sky}} - m_{s_2l}g + k_{u_2l}\left(z_{s_2l} - z_{u_2l}\right) \tag{38}$$

Dynamic modeling of the unsprung mass movement is conducted in two stages. In the first stage; basic dynamic equations for the added unsprung masses m_{u_2r}, m_{u_2l}, and in the second stage, the dynamic equations are considered for the unsprung masses of tires m_{u_1r}, m_{u_1l} in contact with the ground surface.

It must be kept in mind that the terms of $k_{u_2r}\left(z_{s_2r} - z_{u_2r}\right)$ and $k_{u_2l}\left(z_{s_2l} - z_{u_2l}\right)$ are appropriate to exchanged forces to the sprung part and those added to the unsprung part. The two terms are called $F_{(r-s)r}$ and $F_{(r-s)1}$, respectively.

With the second law of Newton for the added unsprung masses, we have:

$$m_{u_2r}\ddot{z}_{u_2r} = -F_{(r-s)r} + F_{u_1r} - m_{u_2r}g + F_{ar_{ground}} \tag{39}$$

$$m_{u_2l}\ddot{z}_{u_2l} = -F_{(r-s)1} + F_{u_1l} - m_{u_2l}g + F_{al_{ground}} \tag{40}$$

As a result:

$$F_{u_1r} = m_{u_2r}\ddot{z}_{u_2r} + F_{(r-s)r} + m_{u_2r}g - F_{ar_{ground}} \tag{41}$$

$$F_{u_1l} = m_{u_2l}\ddot{z}_{u_2l} + F_{(r-s)1} + m_{u_2l}g - F_{al_{ground}} \tag{42}$$

In the same way, for first unsprung masses lead to:
Right tire:

$$m_{u_1 r}\ddot{z}_{u_1 r} = -F_{u_1 r} + F_{tr} - m_{u_1 r}g \tag{43}$$

Left tire:

$$m_{u_1 l}\ddot{z}_{u_1 l} = -F_{u_1 l} + F_{tl} - m_{u_1 l}g \tag{44}$$

By replacing the equations 41 and 42 in the equations 43 and 44, the result is:

$$m_{u_1 r}\ddot{z}_{u_1 r} = -m_{u_2 r}\ddot{z}_{u_2 r} - F_{(r-s)r} - m_{u_2 r}g + F_{ar_{ground}} + F_{tr} - m_{u_1 r}g \tag{45}$$

$$m_{u_1 l}\ddot{z}_{u_1 l} = -m_{u_2 l}\ddot{z}_{u_2 l} - F_{(r-s)1} - m_{u_2 l}g + F_{al_{ground}} + F_{tl} - m_{u_1 l}g \tag{46}$$

Now, for the new model presented in this research, the vertical forces of the tires can be calculated as:

$$F_{tr} = m_{u_1 r}\ddot{z}_{u_1 r} + m_{u_2 r}\ddot{z}_{u_2 r} + F_{(r-s)r} + m_{u_2 r}g + m_{u_1 r}g - F_{ar_{ground}} \tag{47}$$

$$F_{tl} = m_{u_1 l}\ddot{z}_{u_1 l} + m_{u_2 l}\ddot{z}_{u_2 l} + F_{(r-s)1} + m_{u_2 l}g + m_{u_1 l}g - F_{al_{ground}} \tag{48}$$

It is noteworthy that in this stage, a relationship in the forces $F_{(r-s)r}$, $F_{(r-s)1}$, F_{sr_1}, F_{sl_1} should be chosen to be exerted in the rollover index with the 8 degrees of freedom suspension system.

So from the equations 37 and 38, we have:

$$F_{(r-s)r} = F_{sr} + F_{ar_{sky}} + m_{s_2 r}g + m_{s_2 r}\ddot{z}_{s_2 r} \tag{49}$$

$$F_{(r-s)1} = F_{sl} + F_{al_{sky}} + m_{s_2 l}g + m_{s_2 l}\ddot{z}_{s_2 l} \tag{50}$$

By substituting the equations 49 and 50 in the equations 47 and 48, the result is:

$$F_{tr} = m_{u_1 r}\ddot{z}_{u_1 r} + m_{u_2 r}\ddot{z}_{u_2 r} + F_{sr} + F_{ar_{sky}} + m_{s_2 r}g + m_{s_2 r}\ddot{z}_{s_2 r} + m_{u_2 r}g + m_{u_1 r}g - F_{ar_{ground}} \tag{51}$$

$$F_{tl} = m_{u_1 l}\ddot{z}_{u_1 l} + m_{u_2 l}\ddot{z}_{u_2 l} + F_{sl} + F_{al_{sky}} + m_{s_2 l}g + m_{s_2 l}\ddot{z}_{s_2 l} + m_{u_2 l}g + m_{u_1 l}g - F_{al_{ground}} \tag{52}$$

Since the vertical forces of F_{tr}, F_{tl} are equal to those of F_{zr}, F_{zl}, the rollover index, by assuming equality in the mass of the left and right suspension system is:

$$R = \frac{\begin{aligned}&m_{u_1}\left(\ddot{z}_{u_1 r} - \ddot{z}_{u_1 l}\right) + m_{u_2}\left(\ddot{z}_{u_2 r} - \ddot{z}_{u_2 l}\right) + m_{s_2}\left(\ddot{z}_{s_2 r} - \ddot{z}_{s_2 l}\right)\\&+\left(F_{sr} - F_{sl}\right) + \left(F_{ar_{sky}} - F_{al_{sky}}\right) + \left(F_{al_{ground}} - F_{ar_{ground}}\right)\end{aligned}}{\begin{aligned}&m_{u_1}\left(\ddot{z}_{u_1 r} + \ddot{z}_{u_1 l}\right) + m_{u_2}\left(\ddot{z}_{u_2 r} + \ddot{z}_{u_2 l}\right) + m_{s_2}\left(\ddot{z}_{s_2 r} + \ddot{z}_{s_2 l}\right) + \left(F_{sr} + F_{sl}\right)\\&+\left(F_{ar_{sky}} + F_{al_{sky}}\right) - \left(F_{ar_{ground}} + F_{al_{ground}}\right) + 2\left(m_{s_2} + m_{u_2} + m_{u_1}\right)g\end{aligned}} \tag{53}$$

The unknown forces of F_{sr}, F_{sl} cannot readily be measured. This makes it necessary to eliminate the unknown parameters.

To calculate suspension forces $(F_{sr} + F_{sl})$, according to Equation 36:

$$\left(F_{sr} + F_{sl}\right) = m_{s_1} \ddot{z}_{s_1} + m_{s_1} g - \left(F_{ar_{sky}} + F_{al_{sky}}\right) \tag{54}$$

With the rotation equation around the roll center (Equation 35), we have:

$$\left(F_{sr} - F_{sl}\right) = \frac{2}{l_s}\left[-\left(I_{xx} + m_{s_1} h_{R_1}^2\right)\ddot{\phi} + m_{s_1} g\, h_{R1} \sin(\phi) + m_{s_1} a_y\, h_{R1} \cos(\phi)\right] - \left(F_{ar_{sky}} - F_{al_{sky}}\right) \tag{55}$$

Changing the rotational acceleration based on the equation 28 leads to:

$$\left(F_{sr} - F_{sl}\right) = \frac{2}{l_s^2}\left(I_{xx} + m_{s_1} h_{R_1}^2\right)(a_{zr} - a_{zl}) + \frac{2}{l_s}\left(m_{s_1} g\, h_{R1} \sin(\phi) + m_{s_1} a_y\, h_{R1} \cos(\phi)\right) - \left(F_{ar_{sky}} - F_{al_{sky}}\right) \tag{56}$$

By combination of the equations 54 and 56 with the rollover index equation, this index can be applied for the 8 degree of freedom model as:

$$R_{8-DOF} = \frac{\dfrac{2}{l_s^2}\left(I_{xx} + m_{s_1} h_{R_1}^2\right)(a_{zr} - a_{zl}) + \dfrac{2}{l_s}\left(m_{s_1} g\, h_{R1} \sin(\phi) + m_{s_1} a_y\, h_{R1} \cos(\phi)\right)}{\hat{A}}$$

$$+ \frac{m_{u_1}\left(\ddot{z}_{u_1 r} - \ddot{z}_{u_1 l}\right) + m_{u_2}\left(\ddot{z}_{u_2 r} - \ddot{z}_{u_2 l}\right) + m_{s_2}\left(\ddot{z}_{s_2 r} - \ddot{z}_{s_2 l}\right) + \left(F_{al_{ground}} - F_{ar_{ground}}\right)}{\hat{A}} \tag{57}$$

Where

$$\hat{A} = m_{u_1}\left(\ddot{z}_{u_1 r} + \ddot{z}_{u_1 l}\right) + m_{u_2}\left(\ddot{z}_{u_2 r} + \ddot{z}_{u_2 l}\right) + m_{s_2}\left(\ddot{z}_{s_2 r} + \ddot{z}_{s_2 l}\right) + m_{s_1} \ddot{z}_{s_1} - \left(F_{ar_{ground}} + F_{al_{ground}}\right)$$

$$+ 2\left(m_{s_2} + m_{u_2} + m_{u_1} + \frac{m_{s_1}}{2}\right)g \tag{58}$$

4   SIMULATION AND RESULTS OF STABILITY INDEX IN THE CARSIM SOFTWARE

In this section, the results of a simulation of the 4 degrees of freedom suspension system and new models of 6 and 8 degrees of freedom are evaluated in the Carsim software. The selected vehicle in the Carsim software is an SUV for tripped conditions of the rollover. In this model of the car, the mass added to the new system is considered in the Carsim software.

In this study, in order to verify and compare the experimental and analytical laboratory results, all the data used in the new model of the rollover indicators are based on data taken from a reference (Phanomchoeng & Rajamani, 2013).In this regard, the specifications applied to analyze the issue for the 6 and 8 degrees of freedom models are presented in Table 1.

For the implemented model, two kinds of tests are considered. In the first test taken with the Carsim software, the car speed was constant and equal to 80 km/h. Further, the road entrance on the left wheel was equal to 0.15 m. For the second test, the speed was 100 km/h. Also, steering angle input was equal to 1.2 degree and applied since the 1st second. The road input was also equal to 0.15 m/s as a barrier and applied since the 1st second. After setting the parameters for the 6 and 8 degrees models according to what was explained, two modes were examined for each of the tests. In the first case, the parameters of the 6 and 8 degrees models were investigated in accordance with the model drawn in Figures 4 and 8. In the second case, in order to verify the new index investment provided in this article, the added mass quantities were considered as zero-grade. It is expected to practice with the degrees 6 and 8 of the models to make modeling based on a study sample (Phanomchoeng & Rajamani, 2013) and laboratory tests.

4 degrees of freedom	6 degrees of freedom	8 degrees of freedom
		m_{s_1} =1600kg
		$m_{s_2 r}$ =70kg
		$m_{s_2 l}$ =70kg
	m_s =1600kg	$m_{u_1 r}$ =135kg
	$m_{u_1 r}$ =135kg	$m_{u_1 l}$ =135kg
	$m_{u_1 l}$ =135kg	$m_{u_2 r}$ =45kg
m_s =1600kg	$m_{u_2 r}$ =45kg	$m_{u_2 l}$ =45kg
m_{ur} =135kg	$m_{u_2 l}$ =45kg	$k_{s_2 r}$ =70 kN/m
m_{ul} =135kg	k_{sr} =90 kN/m	$k_{s_2 l}$ =70 kN/m
k_{sr} =90 kN/m	k_{sl} =90 kN/m	$k_{u_2 r}$ =20 kN/m
k_{sl} =90 kN/m	k_{ur} =20 kN/m	$k_{u_2 l}$ =20 kN/m
k_{tr} =400 kN/m	k_{ul} =20 kN/m	k_{ur} =20 kN/m
k_{tl} =400 kN/m	k_{tr} =400 kN/m	k_{ul} =20 kN/m
I_{zz} =614kg.m^2	k_{tl} =400 kN/m	k_{tr} =400 kN/m
h_R =1.1m	I_{zz} =614kg.m^2	k_{tl} =400 kN/m
l_s =1m	h_R =1.1m	$d_{s_2 r}$ =2.5 kN.s/m
	l_s =1m	$d_{s_2 l}$ =2.5 kN.s/m
		I_{zz} =614kg.m^2
		h_R =1.1m
		l_s =1m

Table 1: The numerical values used for 4, 6 and 8 degrees of freedom models (Phanomchoeng & Rajamani, 2013).

According to the figure 9, it can be observed that the rollover index with six degrees of freedom in its most negative value is roughly equivalent to the values of the indicators in other studies. In its positive value, it has better performance with a maximum value of 0.18 compared with the values of the indicators in other studies. It is also visible that the indicator model with 8 degrees of freedom in its most negative value as well as a better performance in its most positive value of all indicators. The improvement is more tangible and visible in the process of positive value of the index.
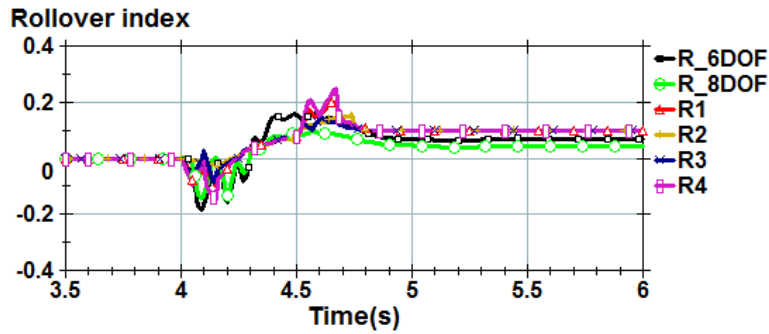
Figure 9: Comparison of the rollover indices: step road input $\left(z_{rl} = 0.15m, v = 80\,Km/h, \delta = 0\right)$.

The result of the comparison of the 6 and 8 degrees of freedom indices with all other indices is represented in Figures 10 and 11, respectively.

As can be seen in Figure 11, the indices of the models with 6 and 8 degrees of freedom have better results compared with those in the study (Phanomchoeng & Rajamani, 2013). It can also be said that the model with 8 degrees of freedom has better performance than that with 6 degrees of freedom.
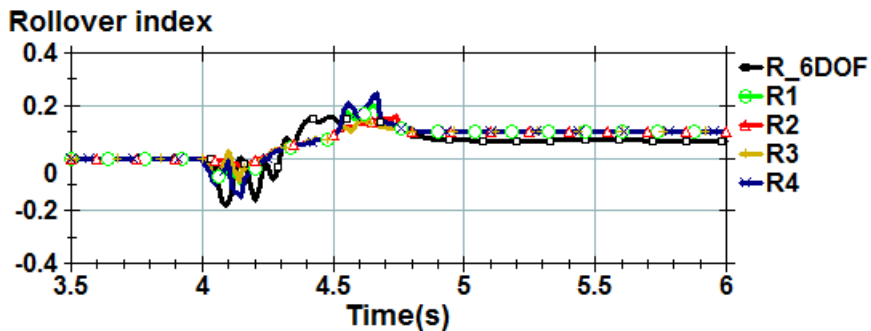
Figure 10: The results of the first test $\left(z_{rl} = 0.15m, \delta = 0\right)$ for 6 degrees of

freedom model with and comparison with the charts in other studies.
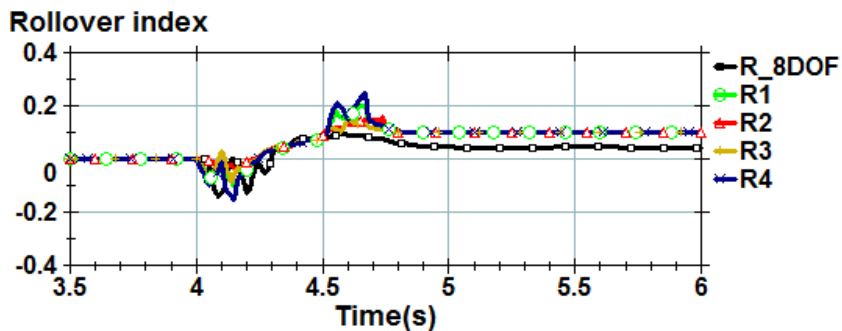
Figure 11: The results of the first test $\left(z_{rl} = 0.15m, \delta = 0\right)$ for model with

8 degrees of freedom and comparison with the charts in other studies.

In follownig, two systems with 6 and 8 degrees of freedom are compared with each other and the results obtained in Rajamani studies.
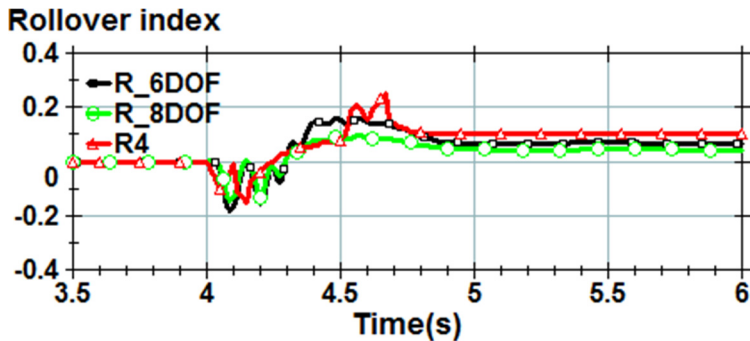
Figure 12: The rollover índices for 6 and 8 degrees of freedom in comparasion with Rajamani index $\left(z_{rl} = 0.15m, v = 80\,Km/h, \delta = 0 \right)$.

The results of the first test for the state with the added mass equal to zero for 6 and 8 degrees of freedom are displayed in Figure 13.

According to Figure 13, it can be observed that in state without the added mass, diagram of six degrees of freedom quite matches the diagram in the rollover index in the 4 degrees of freedom study and the reference laboratory testing (Phanomchoeng & Rajamani, 2013). The index of 8 degrees in addition to full compliance, ranging from 4.3 to 4.7 seconds, has better performance compared with the final performance of the reference index ((Phanomchoeng & Rajamani, 2013)) and its maximum point is lower. This is extremely helpful to vehicle stability.
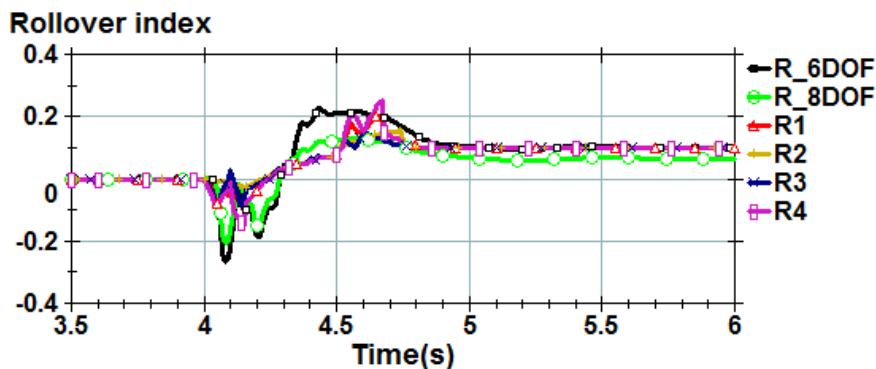
Figure 13: Comparison of rollover indices in state without added mass.

The results of the first test for the state without the added mass with 6 and 8 degrees of freedom are presented individually and in comparison with the chart of all the indicators in Figures 14 and 15, respectively. According to the figure 15, it can be observed that the 8 degrees of freedom model has better performance indicators in equal situations.
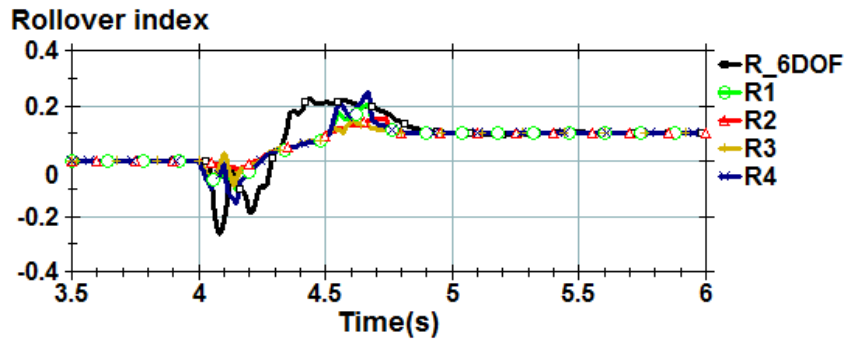
Figure 14: The results of the first test for the state without added mass in models
with 6 degrees of freedom and comparison with the charts in other studies.
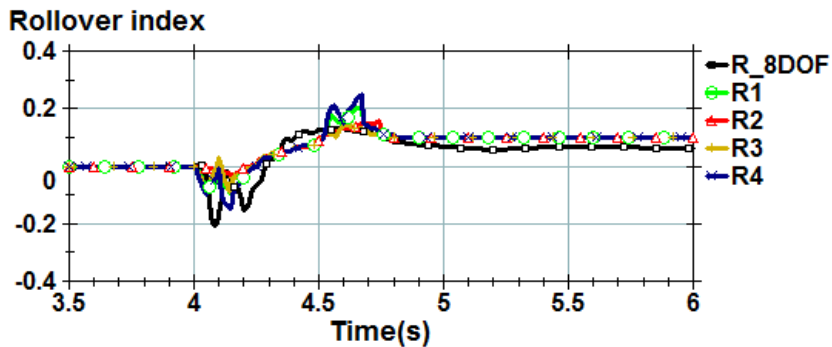
Figure 15: The results of the first test for the state without added mass in models
with 8 degree of freedom and comparison with the charts in other studies.

The Fig. 16 indicates the comparision of results of current study with Rajamini previous studies. It is shown that the obtained results are similar with those appeared in Rajamini studies. The errors that can be seen in Fig. 16 are as the results of ignoring the steering angle in the present study.
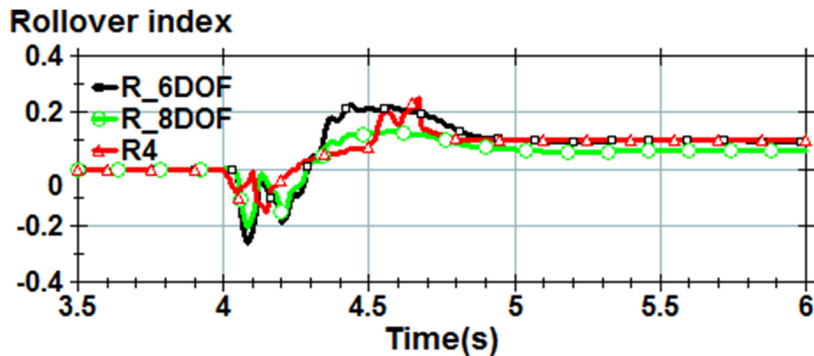
Figure 16: The rollover índices for 6 and 8 degrees of freedom when added masses are equal
to zero and in comparasion with Rajamani index $\left(z_{rl} = 0.15m, v = 80\,Km/h, \delta = 0\right)$.

In this section, results obtained by applying the second test $\left(z_{rl}=0.15m, v=100\,Km/h, \delta=1.2^{\circ}\right)$ are presented. All the arguments in the test 1 can be applied in the test 2. The results and tables indicated that the stability index is improved in the models with 6 and 8 degrees of freedom presented in this study. According to Figure 17, it can be observed that the model of six degrees of freedom in its rate of maximum reaches the value of 0.3. This is while the final value by Rajamani et al. (Phanomchoeng & Rajamani, 2013) was obtained to be 1. Moreover, in their study, other indicators were observed to have more fluctuations relative to the index with 6 degrees of freedom or greater values compared with the index of 8 degrees of freedom. They had also better performance relative to other indices. Thus, the maximum range of the fluctuations of the index is nearly 0.2.
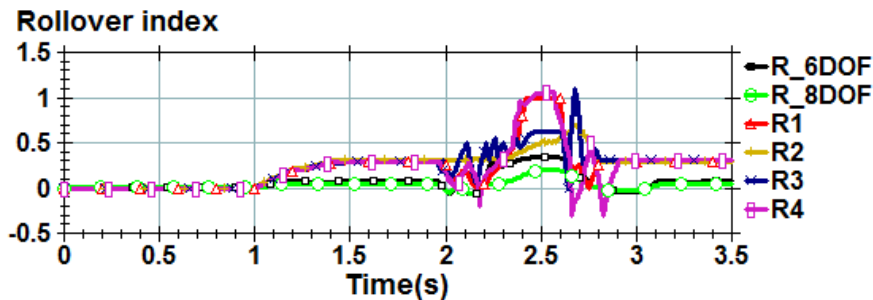
Figure 17: Comparison of rollover indices in second test $\left(z_{rl}=0.15m, \delta=1.2^{\circ}\right)$.

The results of the second test for the state with the added mass in the models with 6 and 8 degrees of freedom and in comparison of the charts R4 ((Phanomchoeng & Rajamani, 2013)) can be observed in Figure 18.

According to Figure 18, it can be observed that the indices of the models with 6 and 8 degrees of freedom have better performance compared with indices in other studies. It also can be observed that the model with 8 degrees of freedom has better performance compared with the model with 6 degrees of freedom.
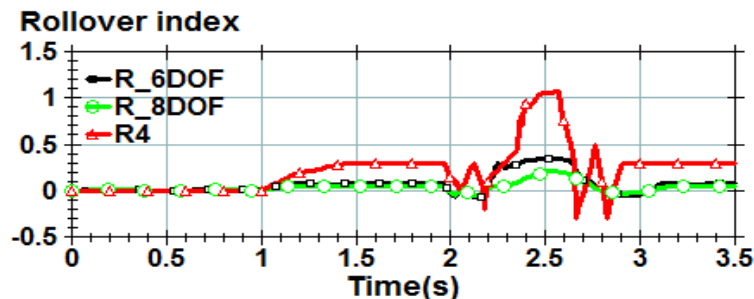
Figure 18: The rollover index in second test $\left(z_{rl}=0.15m, \delta=1.2^{\circ}\right)$ for the model with 6 and 8 degrees of freedom and in comparison with the R4 ((Phanomchoeng & Rajamani, 2013)).

The results of the second test $\left(z_{rl} = 0.15m \,, \delta = 1.2^{\circ} \right)$ for the state with the added mass equal to zero for 6 and 8 degrees of freedom are displayed in Figure 17.

According to Figure 19, results in the state with the added mass equal to zero in the charts with 6 and 8 degrees of freedom confirm the accuracy of the indices and in addition, approve that the charts have better performance relative to the R4 in the study (Phanomchoeng & Rajamani, 2013). Considering the steering angle results in the appropriate compatibility between the Rajamani calculated rollover index with those achieved in the present study.
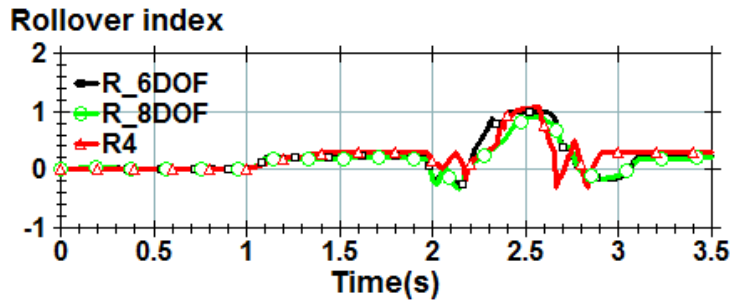
Figure 19: the results of second test for the state without added mass in the models with 6 and 8 degrees of freedom and in comparison with the R4 (Phanomchoeng & Rajamani, 2013).

5   CONCLUSIONS

In this paper, new rollover indices for the models with 6 and 8 degrees of freedom were respectively presented as improved versions of the models with 4 degrees of freedom. The new presented indices were compared with the existing models with 4 degrees of freedom in other studies. This comparison was conducted in the Carsim software as a powerful application for simulation of vehicle systems. After simulation of the three systems of 4, 6, and 8 degrees of freedom in this software and through specific tests according to the scientific findings ((Phanomchoeng & Rajamani, 2013)), improvement in the new stability indices was observed. The good performance of the new system can be easily seen in the first and second tests. The performance improvement in the new systems is high in the moment the tire is detached from the ground surface. This was low in the old system so that the automobile was in the threshold to rollover. In the new model, the stability is in the state when tires are slightly detached from the ground surface. In the first test, the index was obtained about 20% less than other indices. In the second test, the value increased to 60% for the model with 6 degrees of freedom and to 80% for the model with 8 degrees of freedom. It was also specified that the automobile had better stability performance in the 8 degrees of freedom model compared with the 6 and 4 degrees of freedom models.

References

Ahmadian, Mehdi. (2014). Integrating Electromechanical Systems in Commercial Vehicles for Improved Handling, Stability, and Comfort. SAE International Journal of Commercial Vehicles, 7(2014-01-2408), 535-587.

Cech, I. (2000). Anti-roll and active roll suspensions. Vehicle system dynamics, 33(2), 91-106.

Chen, Bo-Chiuan, & Peng, Huei. (1999). A real-time rollover threat index for sports utility vehicles. Paper presented at the American Control Conference, 1999. Proceedings of the 1999.

Dilich, MA, & John, M Goebelbecker. (1997). Truck rollover. Safety Bulletin, Triodyne Inc, 6(1).

Hsu, Ling-Yuan, & Chen, Tsung-Lin. (2012). Vehicle dynamic prediction systems with on-line identification of vehicle parameters and road conditions. Sensors, 12(11), 15778-15800.

Johansson, Björn, & Gafvert, Magnus. (2004). Untripped SUV rollover detection and prevention. Paper presented at the Decision and Control, 2004. CDC. 43rd IEEE Conference on.

Kong, YS, Abdullah, SHAHRUM, Omar, MOHD ZAIDI, & Haris, SALLEHUDDIN MOHAMED. (2016). Topological and topographical optimization of automotive spring lower seat. Latin American Journal of Solids and Structures, 13(7), 1388-1405.

National Highway Traffic and Safety Board, Traffic safety facts. (2011). http://www.safercar.gov/Vehicle+Shoppers/Rollover/Fatalities.

Odenthal, Dirk, Bunte, Tilman, & Ackermann, Jurgen. (1999). Nonlinear steering and braking control for vehicle rollover avoidance. Paper presented at the Control Conference (ECC), 1999 European.

Pagnacco, Emmanuel, Zidani, Hafid, Sampaio, Rubens, de Cursi, Eduardo Souza, & Ellaia, Rachid. (2016). Design Optimization of a Random Suspension Device Considering a Reliability Constraint on the Frequency Response Function. Latin American Journal of Solids & Structures, 13(6).

Pan, Qiang, He, Tian, Xiao, Denghong, & Liu, Xiandong. (2016). Design and Damping Analysis of a New Eddy Current Damper for Aerospace Applications. Latin American Journal of Solids and Structures, 13(11), 1997-2011.

Peters, Steven Conrad. (2006). Modeling, analysis, and measurement of passenger vehicle stability. Massachusetts Institute of Technology.

Phanomchoeng, Gridsada, & Rajamani, Rajesh. (2012). Prediction and Prevention of Tripped Rollovers. Intelligent Transportation Systems Institute Center for Transportation Studies University of Minnesota.

Phanomchoeng, Gridsada, & Rajamani, Rajesh. (2013). New rollover index for the detection of tripped and untripped rollovers. IEEE Transactions on Industrial Electronics, 60(10), 4726-4736.

Rajamani, R, Piyabongkarn, D, Tsourapas, V, & Lew, JY. (2009). Real-time estimation of roll angle and CG height for active rollover prevention applications. Paper presented at the 2009 American control conference.

Rajamani, Rajesh. (2011). Vehicle dynamics and control: Springer Science & Business Media.

Rajamani, Rajesh, & Phanomchoeng, Gridsada. (2013). New rollover index for the detection of tripped and untripped rollovers. IEEE Transactions on Industrial Electronics, 60(10), 4726-4736.

Solmaz, Selim, Corless, Martin, & Shorten, Robert. (2006). A methodology for the design of robust rollover prevention controllers for automotive vehicles: Part 1-Differential Braking. Paper presented at the Proceedings of the 45th IEEE Conference on Decision and Control.

Solmaz, Selim, Corless, Martin, & Shorten, Robert. (2007). A methodology for the design of robust rollover prevention controllers for automotive vehicles with active steering. International Journal of Control, 80(11), 1763-1779.

Solmaz, Selim, Shorten, Robert, Wulff, Kai, & Cairbre, Fiacre O. (2008). A design methodology for switched discrete time linear systems with applications to automotive roll dynamics control. Automatica, 44(9), 2358-2363.

Tavan, Nematollah, Tavan, Mehdi, & Hosseini, Rana. (2015). An optimal integrated longitudinal and lateral dynamic controller development for vehicle path tracking. Latin American Journal of Solids and Structures, 12(6), 1006-1023.

Yoon, Jangyeol, Kim, Dongshin, & Yi, Kyongsu. (2007). Design of a rollover index-based vehicle stability control scheme. Vehicle system dynamics, 45(5), 459-475.